J. Biophotonics **7**, No. 5, 312–322 (2014) / **DOI** 10.1002/jbio.201200135

Journal of BIOPHOTONICS

FULL ARTICLE

Characterisation of a label-free biosensor based on long period grating

Francesco Chiavaioli, Cosimo Trono, Ambra Giannetti, Massimo Brenci, and Francesco Baldini*

IFAC-CNR, Via Madonna del Piano 10, 50019 Sesto Fiorentino, Firenze, Italy

Received 18 July 2012, revised 11 September 2012, accepted 1 October 2012
Published online 6 November 2012

Key words: biochemical sensing, long period grating, flow cell, label-free, immunoassay

Optical fibre gratings, especially long period gratings, have been recently proposed as optical devices for biochemical sensing. A biochemical interaction along the grating portion induces a refractive index change and hence a change in the fiber transmission spectrum. This provides an alternative methodology with respect to other label-free optical approaches, such as surface plasmon resonance, interferometric configurations and optical resonators. The fibre biofunctionalization has been carried out by means of a novel chemistry using Eudragit L100 copolymer as opposed to the commonly used silanization procedure. Antigen-antibody interaction has been analysed by means of an IgG/anti-IgG bioassay. The biosensor was fully characterised, monitoring the kinetics during the antibody immobilization and the antigen interaction and achieving the calibration curve of the assay. A comparison of the biosensor performance was made by using two different long period gratings with distinct periods.

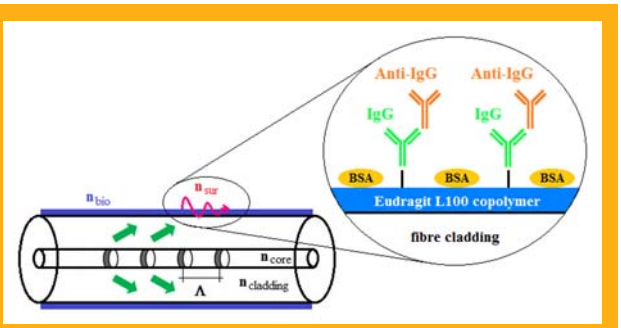

Sketch of the proposed biosensor based on a long period grating. After the deposition of the biolayer, the interaction between the coupled cladding mode and the surrounding environment causes a refractive index change of the layer. The enlargement details the composition of the biolayer.

1. Introduction

In the last ten years, optical fibre sensors (OFSs) saw an impressive growth and progress in the field of research and industry. A special class of OFSs, optical fibre biosensors (OFBs), are drawing more and more the attention of researchers due to the advantages of both an optical approach, which is immune to electromagnetic interferences, and the use of optical fibres, such as the intrinsic miniaturization and the easy integration in an optical fibre network for multiple site monitoring. Broadly speaking, a chemical/biochemical interaction along the fibre induces a change in the optical properties of the medium surrounding the fibre. One of the most interesting parameter, which is affected by these interactions, is the refractive index (RI). A change in RI can be evaluated by means of optical approaches, such as surface plasmon resonance (SPR), interferometric configurations manufactured on both optical fibres and wave-

* Corresponding author: e-mail: c.trono@ifac.cnr.it, Phone: +39 055 522 6359, Fax: +39 055 522 6400

guides, and optical resonators (ORs). Technology platforms based on SPR are the most widespread ones [1], but also those based on the other optical approaches are surely appealing, since the resolution in terms of RI units (RIU) can be comparable with SPR, if not few orders of magnitude better [2]. Measurement of RI changes gives the chance to directly detect biochemical species without resorting to luminescence- or absorption-based measurements. In fact, the use of labelled techniques many times implies multistep detection protocols (e.g. ELISA, sandwich assays, etc.), which can be more difficult in terms of sample manipulation and time-consuming. On the contrary, a label-free technique does not exhibit these problems and allows performing real time measurements of the biochemical interaction between the analyte and the deposited biolayer, thus giving also the opportunity to study the kinetics of interaction.

In the last years, optical fibre gratings (OFGs) have been proposed as effective tools for chemical and biochemical sensing [3–5]. The applications in the biochemical field are really manifold, ranging from the detection of DNA target [6], antibody-antigen interaction [4, 7, 8], biotin-streptavidin pair [9], and specific bacteria using bacteriophages [10]. The use of OFGs can offer some advantages with respect to other optical technologies thanks not only to the above mentioned typical advantages of the optical fibres, but also to their high compatibility with optoelectronic components/devices used for telecommunication applications, since the resonance wavelength lies within the 1.3 μm and 1.5 μm optical telecommunication windows. In addition, the use of OFGs provides multiplexing and remote measurement capabilities, since the signal modulation is spectrally encoded. The combination of multiplexing/remote monitoring should not be underestimated: the possibility of having along the same fibre different sensing points for different bioanalytes is undoubtedly peculiar of optical fibres and cannot be easily achieved with other label-free approaches.

An OFG is a periodic modulation of the core refractive index of a single-mode fibre (SMF). The literature accounts for two types of OFGs according to the period of the modulation (i.e. grating period Λ). The former are known as fibre Bragg gratings (FBGs), which are characterised by a grating period in the order of hundreds of nanometres and a phase matching condition (PMC) between the fundamental core mode and its respective counter-propagating mode. The latter are known as long period gratings (LPGs), which are characterised by a grating period in the order of hundreds of micrometres and a PMC between the fundamental core mode and a discrete set of forward-propagating cladding modes. The specific coupling between the modes verifying the PMC generates in the transmission spectrum of the fibre a series of attenuation bands centred at discrete wavelengths (i.e. resonance wavelengths λ_{res}).

Vengsarkar et al. [11] and Hill et al. [12] first reported the operating principle and the main characteristics of LPGs and FBGs, respectively. Starting from the PMC of the two gratings, not explicitly shown but easily found in Ref. [13], the shift of the resonance wavelength $\Delta\lambda_{res}$ can be expressed in terms of changes in strain and temperature for the FBGs, but also in RI of the medium surrounding the fibre for the LPGs, due to the interaction between the core and cladding modes. It is this dependence on the external RI that makes LPGs a promising platform for biosensing.

For the sake of completeness, FBGs can also be used as surrounding RI (SRI) sensors by means of the alteration of the fibre structure (i.e. etched FBGs) or the grating geometry (i.e. tilted FBGs) [3]. In both cases, anyway, the obtained values of RI sensitivity are lower than those obtained using LPGs, except for FBGs with a deep etching over the fibre core [14], nevertheless to the detriment of the mechanical strength of the entire structure.

It is worth highlighting that the LPG sensitivity to refractive index is influenced by both the grating period and the order of the coupled cladding mode, since the PMC of LPGs is dependent on both Λ and the difference between core and cladding effective refractive indexes (ERI), which, in turn, depends on the SRI [15]. As the refractive index of the medium surrounding the grating portion changes, a shift of the LPG λ_{res} is expected. In general, the maximum RI sensitivity is attained when the SRI approaches the value of the fibre cladding (i.e. 1.455 RIU). Because bioassays are carried out in aqueous solution (i.e. 1.333 RIU) in a range where the RI sensitivity is low [15], the problem can be overcome by means of the deposition of an overlay of higher RI (ranging from 1.5 RIU to 1.7 RIU) than that of the fibre cladding on the LPG portion [5, 16, 17]. On the other hand, our approach, the deposition of a selective biolayer onto the LPG surface provides the simple manner for carrying out a feasibility study of a biosensor based on OFGs, without resorting to more complicated four-layer structures and additional chemical treatments of the optical fibre.

The use of OFGs in the biochemical field has pointedly advantages and limitations [3], but represents certainly a ground-breaking technology in the field of research. However, there are some issues that have to be pointed out concerning the biochemical sensing, especially if it is based on OFGs. Firstly, it is necessary to have stable conditions of the measuring environment, although it is not enough. In fact, because of the influences of LPG cross-sensitivities, it is crucial to have a reliable and effective thermal and mechanical stabilisation of the entire system in order to accurately measure very low changes in

RI as occurs in bioassays [18]. Secondly, it is worth highlighting a general concept about RI measurements, that is the difference between bulk measurement and surface measurement. The former takes into account the interactions occurring all around the fibre and hence in the volume of the liquid. Differently, the latter just takes into account the interactions occurring in the layer deposited on the fibre. This distinctiveness is significant and fundamental in order to quantitatively measure the amount of analyte under study, which selectively interacts with biological recognition elements (BREs) covalently bonded to the fibre surface. An overall view and a comparison about the performances of chemical and biochemical sensors based on optical fibre gratings is given in references [3, 19].

Starting from a previously published work [18], in which the design and characterisation of a thermo-stabilised flow cell of relatively low-volume (tens of μL) have been fully described for accurate refractive index measurements using an LPG and a methodology for measuring and correcting all the sensor cross-sensitivities, we demonstrate that the same system can be successfully used in the field of biochemical sensing. In this paper, we present a feasibility study of a label-free LPG-based biosensor with the implementation of the complete calibration curve, thanks to the use of a platform perfectly stabilised and/or automatically compensated in terms of small changes of temperature and strain. Moreover, for the first time, the chemistry using Eudragit L100 copolymer [20] has been tested for the fibre biofunctionalization besides the commonly used silanization procedure [21]. Finally, to give a comparison of the biosensor performance and thus to improve its metrological parameters, the same bioassay procedure has been carried out twice using two different LPGs with distinct periods.

2. Experimental

2.1 Reagents

Ethanol (EtOH), bovine serum albumin (BSA), phosphate-buffered saline (40 mM PBS, pH 7.4) were purchased from Sigma, Sigma-Aldrich S.r.l., Milan, Italy. The methacrylic acid/methacrylate copolymer (Eudragit L100) was purchased from Degussa, Röhm Pharma Polymers, Evonik Degussa GmbH, Düsseldorf, Germany. The mouse IgG, goat anti-mouse IgG and Cy5-labelled goat anti-mouse-IgG were purchased from Zymed Laboratories, Invitrogen Immunodetection, Milan, Italy. 1-Ethyl-3-[3-dimethylaminopropyl] carbodiimide hydrochloride (EDC) and N-hydroxysuccinimide (NHS) were purchased from Pierce, Rockford, Illinois, USA. Mouse monoclonal antibody, anti-PSA (prostate-specific antigen), clone A67-B/E3, was kindly provided by EXBIO Praha, Czech Republic.

2.2 Optical measuring setup

The proposed RI sensing system is made up of a hybrid cascaded configuration of OFGs placed inside a thermo-stabilised flow cell. The LPG is used as RI sensor, whereas the FBG is used as strain sensor. Furthermore, a thermocouple inserted as close as possible to the flow channel and connected to a thermometric measuring unit (Lutron TM-917) is used as temperature sensor of the entire system.

By measuring both λ_{res} of the two gratings and the temperature, the strain and temperature changes and/or fluctuations can be compensated [18] and an accurate value of LPG $\Delta\lambda_{res}$ as a function of a change in surrounding RI can be obtained.

The flow cell is accurately described in Ref. [18]. Shortly, it is constituted by two parts, the upper in PMMA and the bottom in aluminium. The flow channel (square cross section of 1 mm^2, 50 mm long) is manufactured by means of two grooves implemented on the two parts and the total volume of the flow channel is 50 μL. Furthermore, an open cell was manufactured to evaluate the effectiveness of the functionalization of the fibre surface (see Section 3). The open cell consists of a u-groove made on a piece of polytetrafluoroethylene (PTFE). The piece of PTFE is 70 mm long and 7 mm wide and high, whereas the u-groove was manufactured in the centre of the PTFE piece and is 50 mm long and 2 mm wide and high. In addition, a 0.4 mm deep v-groove is engraved on the ends of the PTFE piece in order to fix the optical fibre, which is glued with its jacket to the v-groove edges using an UV optical flexible adhesive (Norland 65).

The schematic block diagram of the entire optical measuring setup is shown in Figure 1. A superluminescent diode (SLD, INPHENIX IPSDD1503) with its maximum wavelength centred at 1550 nm is used as optical source; an optical spectrum analyser (OSA, Anritsu MS9030A and MS9701B) allows to measure the λ_{res} of the two gratings and a peristaltic pump (Gilson MINIPULS 3) connected to the flow cell by means of F117938 PVC tubing makes it possible to pump solutions into the flow cell with a given flow rate. The data acquisition is carried out by means of the RS-232 serial interface for the temperature and the GPIB interface for the λ_{res} of the two gratings (see Figure 1), whereas the data processing makes use of an in-house developed NI CVI program. The software routine, first for the LPG and then for the FBG, acquires the spectrum

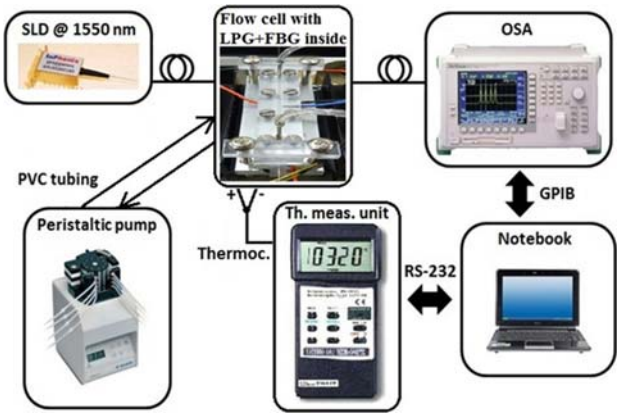

Figure 1 Schematic block diagram of the proposed measuring setup.

and extrapolates and saves the minimum wavelengths by means of an ad-hoc developed data fitting, which makes use of a Lorentzian function for the LPG and a Gaussian one for the FBG. The developed software allows also to acquire the temperature value and the total acquisition time is about 23 s [18].

Concerning the manufacturing of both FBGs and LPGs on a photosensitive boron-germanium co-doped optical fibre (Fibercore PS1250/1500), two different methods are used. FBGs are inscribed using the well-known method of the phase mask [22] with an excimer KrF laser (LAMBDA PHYSIC COMPex 110) and are characterised by a length of 1 cm and λ_{res} in the range of 1533–1534 nm. Other manufacturing parameters are the fluence per pulse, 450 mJ cm^{-1}, the total writing time, 1 minute, and the total number of laser shots, around 3000. On the other hand, LPGs are inscribed by a point-to-point technique, using the same laser source but with a different experimental setup, which makes use of a micrometric slit for the beam shaping and a cylindrical lens for the beam focusing [18]. By changing both the step of the computer-controlled translation stage and the width of the micrometric slit, it is possible to choose Λ and hence the order of the coupled cladding mode, which influences the spectral response of LPGs and, in turn, the device sensitivity [23]. Two different LPGs were manufactured with grating periods of 615 μm (LPG A) and of 370 μm (LPG B). In both cases, a fluence per pulse of about 300 mJ cm^{-2} was used, whereas the total writing time and the total number of laser shots were 20 minutes and 60 000 for LPG A and 13 minutes and 38000 for LPG B. The optical characteristics of LPG A and LPG B are collected in Table 1.

Table 1 Optical characteristics of LPG A and LPG B.

Sample	λ_{res} in air (nm)	Cladding mode order	Grating length (cm)
LPG A	1567	4-th	2.46
LPG B	1553.5	7-th	2.035

After the grating manufacturing, the fibre portion containing the two gratings is placed inside the thermo-stabilised flow cell and is fully characterised with respect to the influences of the cross-sensitivities, i.e. strain and temperature. By applying the procedure to eliminate the effects of both strain and temperature on the LPG-based RI sensor, as detailed in Ref. [18], the proposed system can be used for accurate RI measurements in the biochemical field.

Fluorescence measurements were performed to evaluate the homogeneity of the biochemical layer deposited on the fibre (see Section 3). The fluorescence emitted by the deposited layer was measured by using a focused laser diode light at 635 nm as excitation source and a plastic optical fibre (POF), perpendicular to the fibre axis and forming an angle of 45° with respect to the excitation beam, which collects the emitted fluorescence and send it to a spec-

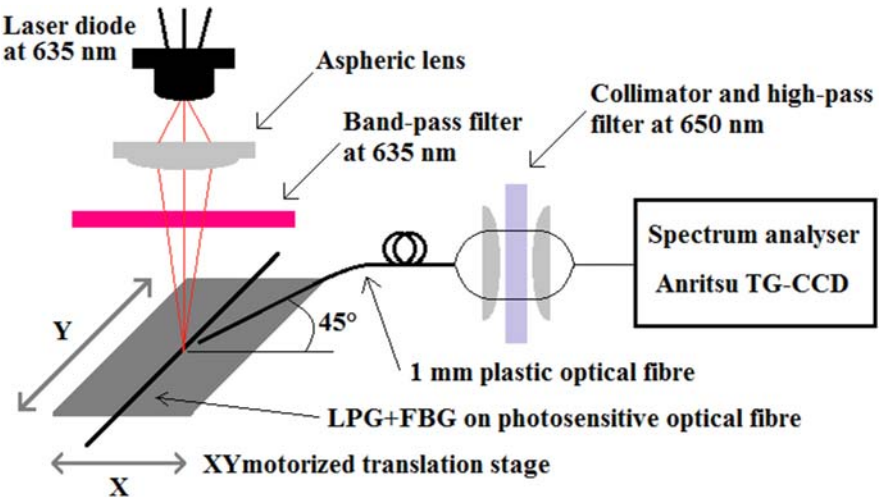

Figure 2 Sketch of the fluorescence measuring setup.

trum analyser (Anritsu TG-CCD). A computer-controlled XY motorized translation stage allows scanning the optical fibre under test along its length. The sketch of the fluorescence measuring setup is depicted in Figure 2.

2.3 Chemical treatment of LPGs and bioassay protocol

LPG surfaces were functionalised by immersion in 2 mM Eudragit L100 copolymer in ethanol for 1 minute and then waiting about 15 minutes in air, until the complete solvent evaporation occurred. The polymeric deposition provides carboxylic functional groups (−COOH) to the surfaces, useful for antibody immobilization. Once the LPGs were functionalised, fibres were collocated into the flow cell and all the following steps were performed for the preparation of the biological sensing layer:

i) activation of −COOH groups by means of EDC (2 mM) and NHS (5 mM) for 30 minutes;
ii) immediate covalent immobilization of the antibodies on the LPG surface, by pumping a solution of 1000 mg L^{-1} mouse IgG in PBS for 1 hour;
iii) washing with PBS buffer to remove the unreacted IgG for 5 minutes;
iv) surface passivation with 3% BSA in PBS for 15 minutes in order to reduce/eliminate the non-specific adsorption on the fibre surface.

All this procedures were carried out with a careful control of the temperature, keeping the external temperature at 25 °C and the flow cell temperature at 23 °C [18].

The non-specific interaction with the IgG layer was tested pumping a solution of PBS containing 10 mg L^{-1} of anti-PSA in the flow cell. Bioassays were then performed with different concentrations of goat anti-mouse IgG (0.1−500 mg L^{-1}) following the developed protocol, with 15 minutes of incubation time for the antigen and 5 minutes for PBS washing step.

As for fluidics, two different flow rates were used:

– 250 μL min^{-1} for surface activation and passivation and for all the washings in PBS;
– 25 μL min^{-1} for the immobilization of mouse IgG, the non-specific interaction with anti-PSA and the implementation of the assay with goat anti-mouse IgG.

The sketch of immunoassay performed on the biofunctionalised fibre is shown in Figure 3. The figure illustrates the RI sensing principle: after the deposition of the biolayer, the interaction of light travelling in the fibre cladding (green arrows), which is related to the coupled cladding mode, with the surroundings generates an evanescent wave (pink wave) and causes a change of the optical properties of the layer itself. The most interesting feature is doubtless the RI change of the biolayer due to the antibody-antigen bond occurred. Moreover, the enlargement of the figure gives a schematic representation of the biolayer composition, starting from the deposition of a thin polymeric layer (sky-blue) in order to give free −COOH groups, useful for antibody immobilization by means of EDC/NHS cross-linkers activation, carrying on with both the surface passivation by means of BSA (dark-yellow ovals) and the mouse IgG antibody immobilization (light-green), and closing with the interaction with the specific goat anti-mouse IgG (orange).

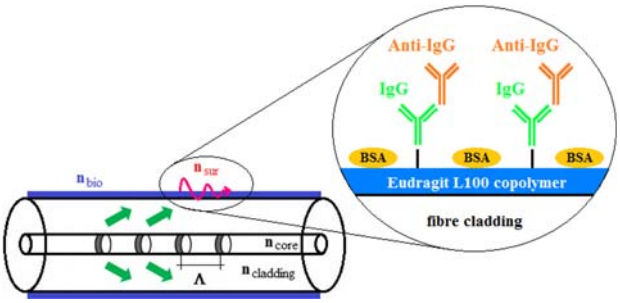

Figure 3 Sketch of the proposed biosensor based on a LPG. After the deposition of the biolayer, the interaction between the coupled cladding mode and the surrounding environment causes a RI change of the layer. The enlargement gives a schematic representation of the biolayer composition. n_{bio} is the RI of the deposited biolayer, whereas n_{sur} is the RI of the surrounding environment.

3. Results and discussion

Firstly, the effect of functionalization of the LPG surface with Eudragit L100 copolymer [20], besides the commonly used silanization procedure [21], was carefully investigated. With this purpose, the changes in the LPG resonance wavelength were continuously monitored during this chemical process of functionalization using the open cell described in Section 2.2, on which the optical fibre with the embedded FBG and LPG was fixed.

Figure 4 shows the changes of the LPG resonance wavelength during the whole process. Two different cycles can be observed. In the first cycle the flow cell was filled with pure ethanol, whereas in the second cycle it was filled with Eudragit L100 in ethanol.

In this way it was possible to exactly identify the changes due to a simple evaporation process of the solvent and the effect coming from the formation of the Eudragit L100 layer on the fibre surface. The total evaporation time is about 45 minutes for both cycles and three distinct events can be distinguished.

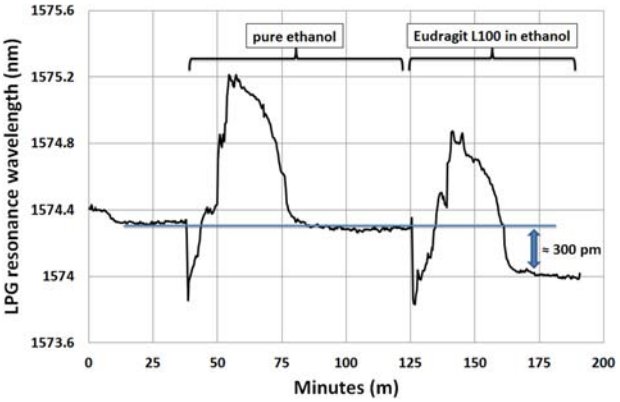

Figure 4 LPG resonance wavelength vs. time in the presence of pure ethanol and in the presence of a Eudragit L100 solution in ethanol.

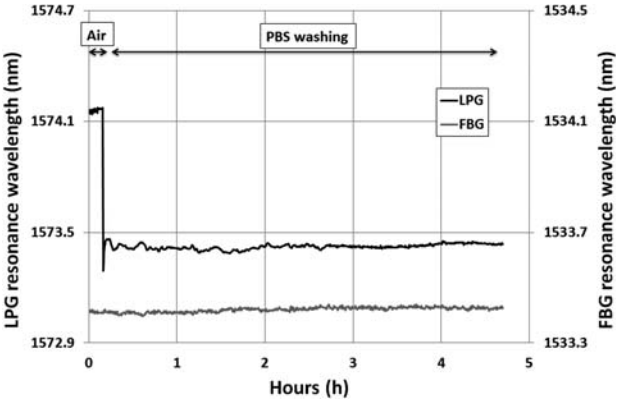

Figure 5 Stability test on the LPG B λ_{res} (black line) and on the FBG λ_{res} (grey line) after the deposition of Eudragit L100 copolymer by pumping a PBS solution at constant rate of 250 μL min^{-1}. At $t = 10$ min, the stability test starts and the SRI changes from 1 RIU of air to 1.334 RIU of PBS washing solution.

The first event is characterised by a decrease of the LPG λ_{res} that occurs outright due to a change of the external RI related to the ethanol. The second event, whose time is about 20 minutes, is characterised by an increase of the LPG λ_{res}, which is ascribed to a temperature decrease due to the evaporation process of ethanol inside the open cell. Afterwards, the last event, whose time is about 25 minutes, is characterised by a decrease of the LPG λ_{res}, which is ascribed to a temperature increase up to the environmental temperature, as in the beginning of the measurement. It is worth highlighting that the value of the LPG λ_{res} remains unchanged after the complete evaporation of pure ethanol, whereas it decreases of about 300 pm after the deposition of Eudragit L100 copolymer in ethanol, providing the evidence of the deposition of a thin layer onto the grating region.

The measurement of the stability of the deposited copolymer layer was carried out by placing the optical fibre inside the manufactured flow cell [18] and by pumping a PBS solution at constant rate of 250 μL min^{-1} for more than 4 hours. The obtained results are detailed in Figure 5 by monitoring the resonance wavelengths of LPG B (black line) and FBG (grey line). It can be seen that both the λ_{res} remained practically constant with a standard deviation of 13 pm for LPG B and 8 pm for FBG. This guarantees the efficacy of the proposed functionalization chemistry using Eudragit L100 copolymer. As expected, the FBG λ_{res} is completely insensitive to the changes in external refractive index.

The coverage of the optical fibre after the antibody-antigen interaction was controlled by performing the first bioassay that made use of labelled goat anti-mouse IgG. After the immobilization of mouse IgG according to the previously described protocol, 10 mg L^{-1} Cy5-labelled goat anti-mouse IgG in PBS was pumped into the flow cell for 15 minutes. After a washing step of 5 minutes in PBS, the measurement of the fluorescence emitted by the deposited layer was carried out by means of the setup described in the previous section (see Figure 2).

Figure 6 shows the fluorescence measured by scanning a 3 cm long portion of the fibre. For the sake of clarity, this grey-level figure is not a picture, but it is a simple software reconstruction of the fluorescence measurement in which the brightness of each pixel is directly proportional to the intensity of the emitted fluorescence. Except for a slight misalignment of the fibre with respect to the translation stage, the emitted fluorescence is uniform enough to confirm that the antibody-antigen interaction occurred quite homogeneously all around the fibre. It should be noted that the evaluation of the homogeneity of the biolayer is carried out at the micron scale, since the step of the translation stage is 50 μm and the core diameter of the plastic fibre with which the fluorescence signal is collected is equal to 1 mm, but this information can be considered sufficient to show that an homogeneous layer is formed along the whole fibre surface.

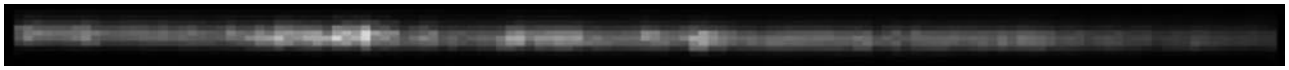

Figure 6 Measurement of the fluorescence emitted by the layer deposited on the optical fibre (LPG A) after the implementation of the bioassay carried out with Cy5-labelled goat anti-mouse IgG.

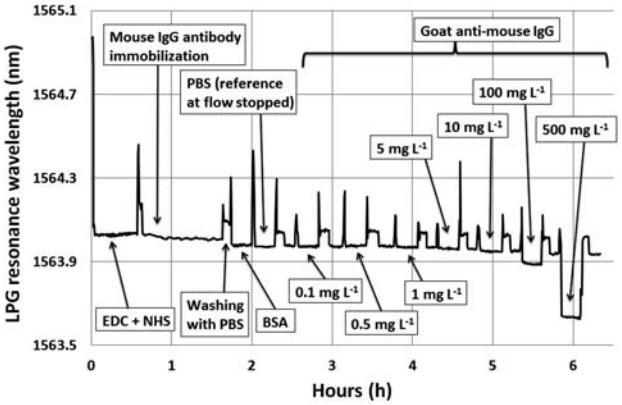

Figure 7 Response curve of the sensor for the bioassay using LPG A. The first 2 hours are related to the i)–iv) steps described in Section 2.3 for the preparation of the IgG sensing layer. The other part of the response curve is related to the exposure to different concentrations of goat anti-mouse IgG, ranging from 0.1 mg L^{-1} to 500 mg L^{-1}.

After this check, all the subsequent bioassays were performed using label-free goat anti-mouse IgG. Figures 7 and 8 show the response curve for the bioassay carried out with LPG A and LPG B, respectively. By continuously monitoring the LPG resonance wavelength with the measuring setup described in Section 2.2, all the measurement steps of the protocol described in Section 2.3 can be followed in real time.

Each step of the protocol described in the previous section is indicated by an arrow and a text box that specifies both the reagents and their concentrations. The duration of the whole measurement is of several hours, but the long-term stability of the whole system (six hours stability test, 7 pm standard deviation and 1.5 pm h^{-1} of drift for the LPG λ_{res} at

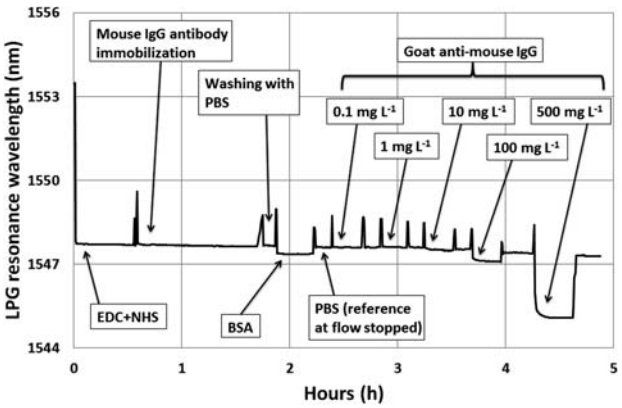

Figure 8 Response curve of the sensor for the bioassay using LPG B. The first 2 hours are related to the i)–iv) steps described in Section 2.3 for the preparation of the IgG sensing layer. The other part of the response curve is related to the exposure to different concentrations of goat anti-mouse IgG, ranging from 0.1 mg L^{-1} to 500 mg L^{-1}.

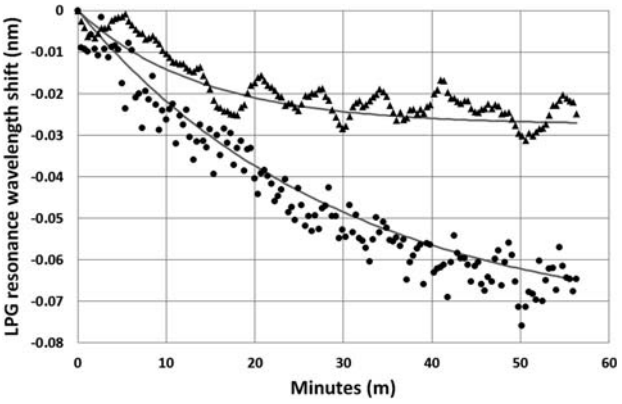

Figure 9 Resonance wavelength vs. time during the mouse IgG antibody immobilization on the fibre surface, carried out on LPG A (black triangles) and on LPG B (black circles). The solid grey lines represent the best exponential curve fitting of the experimental data.

the end of the measurement), successfully tested and deeply discussed in Ref. [18], assures the absence of undesired drifts. All the spikes showed in the response curves are related to a quick and fast passage of air into the flow channel between two subsequent solutions in order to avoid the formation of air bubbles, which can alter the RI measurement.

The kinetics of the immobilization of mouse IgG antibody onto the fibre surface is shown in Figure 9, which accounts for the shifts of the λ_{res} as a function of the time for both LPG A and LPG B. For an easy comparison, the initial value of the λ_{res} is shifted to zero, with the first three experimental data excluded in order to discard the contribution coming from the volume RI change.

The total shift of the λ_{res} detected in LPG B (black circles) is about three times larger than the shift measured in LPG A (black triangles), as expected due to the greater sensitivity of the LPG B in terms of RI changes. Figure 9 shows also the fitting (solid grey lines) of the experimental data with the exponential function

$$y = y_0 + A_1 e^{-\left(\frac{x}{t_1}\right)} \quad (1)$$

for both the LPGs. The values of the constants of the exponential function for both the gratings are collected in Table 2 along with the correlation coefficients, the maximum deviation of residuals and the total shift of the resonance wavelengths. The values of the fitting function given in Table 2 are related to the measured values of the λ_{res} showed in Figures 7 and 8 and not to the normalized $\Delta\lambda_{res}$ values shown in Figure 9. The dispersion of the experimental data around the exponential fitting can be overestimated by means of the maximum deviation of residuals, which is 14 pm for LPG A and 19 pm for LPG B. These values give an idea of the uncertainty on a single experimental point, which is of the order of

Table 2 Comparison of the results achieved with LPG A and LPG B in the case of the immobilization of mouse IgG antibody on LPG A and on LPG B.

Parameter	LPG A	LPG B
y_0 (nm)	1564.007 ± 0.001	1547.6273 ± 0.003
A_1 (nm)	0.028 ± 0.001	0.0764 ± 0.002
t_1 (m)	14.7 ± 1.4	29.8 ± 2.4
correlation coefficient	0.82	0.95
maximum deviation of residuals (nm)	0.014	0.019
total $\Delta\lambda_{res}$ (nm)	0.026	0.065

5 pm–10 pm, in good agreement with the standard deviation measured in the stability test and in the statistical evaluation of experimental points showed later into the calibration curves.

It is worth remembering that the important measurand is constituted by RI changes induced along the functionalised surface due to the interactions between the immobilized antibody and the specific antigen, and not by bulk RI changes, simply related to the refractive index of the solutions, which are pumped inside the flow cell. This means that a washing step with PBS is necessary after each addition of goat anti-mouse IgG in order to measure the real shift of the LPG λ_{res}, caused by the antibody/antigen interaction on the fibre surface. Figure 10 shows the enlargement of the response curve in case of the addition of 100 mg L^{-1} for LPG B, with the clear indication of the measured λ_{res} shift.

As expected, the antibody-antigen interaction induces an increase of the effective refractive index of the coupled cladding mode, which, in turn, causes a decrease of the LPG resonance wavelength (see the LPG characteristic equation given in Ref. [13]). This effect can be explained considering an increase in both the thickness and the average refractive index of the deposited biolayer. In addition, there is another interesting feature that is worthy to be mentioned: after the exposure to the blocking solution (BSA) and the subsequent PBS washing step, the value of LPG resonance wavelength is different from the previous one, associated with the immobilization of mouse IgG antibody. This is a clear indication that the surface passivation is necessary in order to avoid non-specific absorption during the implementation of the assay.

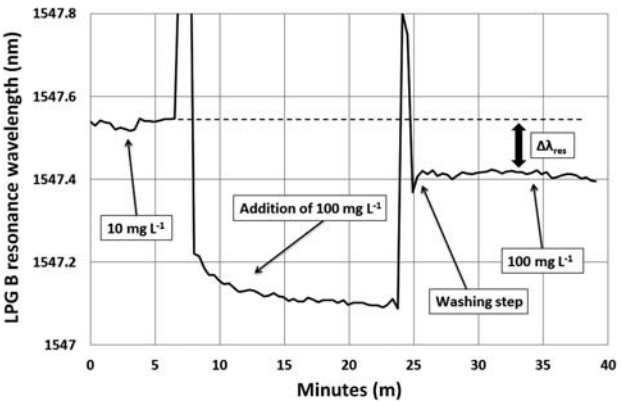

Figure 10 Shift of the LPG B resonance wavelength vs. time after the addition of 100 mg L^{-1} goat anti-mouse IgG.

As can be seen in Figures 7 and 8, the bulk response to 100 and 500 mg L^{-1} of goat anti-mouse IgG is sensibly higher compared to the response to the other concentrations. This is due to the composition of the preservative solution of the goat anti-mouse IgG constituted by a solution of 40% glycerol in buffer. With the increase of the concentration of the goat anti-mouse IgG, the contribution of glycerol to the volume RI change becomes more and more evident and is clearly visible for the two higher concentrations (100 and 500 mg L^{-1}). Obviously, after the washing steps, this bulk-effect is completely removed and the resulting shift of the LPG λ_{res} is only related to the antibody/antigen interaction. For the sake of completeness, the LPG B exhibits a volume RI sensitivity of 15 nm RIU^{-1} around 1.33 RIU.

By analysing the response curves of Figures 7 and 8, it is possible to plot the calibration curve of the biosensor by drawing the concentration of each goat anti-mouse IgG (antigen) as a function of the shift of the LPG λ_{res}. The value of each experimental point is given by the average of 15 values measured stopping the flow after each PBS washing step. Figure 11 shows the calibration curve of the bioassay performed with LPG A. The corresponding standard deviation of each experimental point was also calculated and showed in the figure as black error bars with a mean value of the order of 10 pm. The dot on

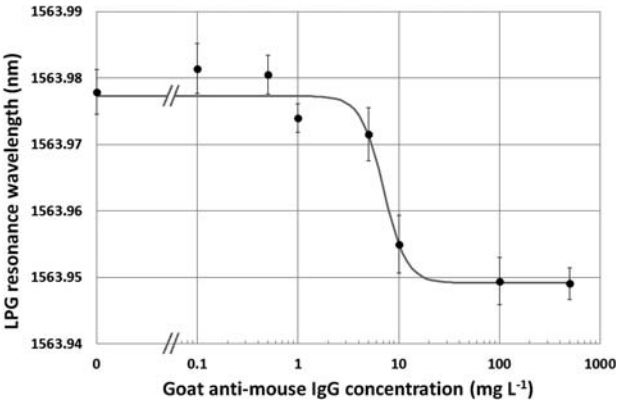

Figure 11 Calibration curve of the bioassay carried out with LPG A. Each experimental point (black circles) is the average of 15 subsequent measurements and the respective standard deviations (black error bars) are also shown. The solid grey line provides the best sigmoidal curve fitting of the experimental data.

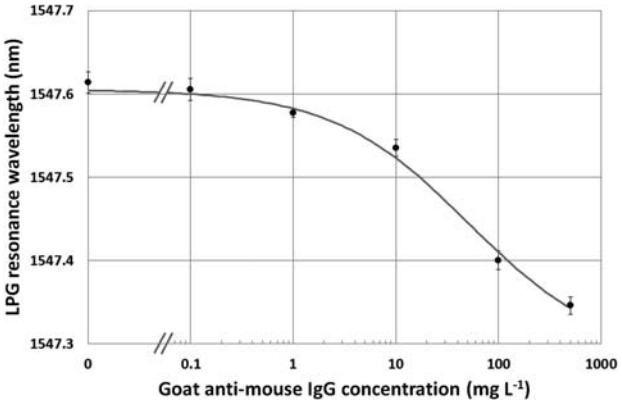

Figure 12 Calibration curve of the bioassay carried out with LPG B. Each experimental point (black circles) is the average of 15 subsequent measurements and the respective standard deviations (black error bars) are also shown. The solid grey line provides the best sigmoidal curve fitting of the experimental data.

the y-axis is the measured value of the λ_{res} taken in PBS before the exposure to any goat anti-mouse IgG concentration.

The fitting with the logistic function

$$y = F_{min} + \frac{F_{MAX} - F_{min}}{1 + (x/x_0)^p} \quad (2)$$

is also shown, where F_{MAX} and F_{min} are the asymptotes of the sigmoidal curve and their difference represents the dynamic signal change of the LPG λ_{res} (hereafter named dynamic signal range), x_0 is the value of the antigen concentration for which the value of LPG resonance wavelength is equal to 50% of the dynamic signal range, and p is a coefficient that is related to the slope of the sigmoidal curve and is calculated for $x = x_0$. This function is a well-accepted mathematical model for describing the sigmoidal curve [24].

The quality of the fitting is very bad, with a correlation coefficient of 0.94 and this is to be ascribed to the low sensitivity of the biosensor, as clearly highlighted by the large error bars that are up to one fourth of the total signal change.

Different is the case of the calibration curve of the bioassay performed with LPG B and shown in Figure 12, which is characterised by a noticeable better sensitivity due to the shorter period of the grating.

In Table 3 the fitting parameters are given for both the gratings (A and B) along with the correlation coefficient, the dynamic signal range (DSR), the working range (WR) and the limit of detection (LOD) of the biosensor. The working range of the biosensor can be calculated considering the antigen concentration range between 10% and 90% of the dynamic signal range ($F_{MAX} - F_{min}$) [25], whereas the limit of detection was evaluated following the International Union of Pure and Applied Chemistry rules, as three times of the standard deviation of the blank measurement, i.e. the measurement achieved with buffer [26].

Table 3 Comparison of the results obtained with LPG A and LPG B.

Parameter	LPG A	LPG B
	Value and related standard deviation	Value and related standard deviation
F_{MAX} (nm)	1563.972 ± 0.006	1547.605 ± 0.015
F_{min} (nm)	1563.944 ± 0.009	1547.283 ± 0.067
x_0 (mg L^{-1})	7.1 ± 1.4	51.5 ± 41.2
p	3.81 ± 2.07	0.65 ± 0.21
correlation coefficient	0.94	0.98
DSR (nm)	0.028	0.322
WR (mg L^{-1})	4.0–12.6	1.7–1450
LOD (mg L^{-1})	7.6	0.5

Compared to the bioassay performed with LPG A, in which the grating has a period of 615 μm and thus the coupling occurs with a low-order cladding mode (4-th), the DSR attained with the bioassay performed with LPG B, in which the grating has a period of 370 μm and thus the coupling occurs with a higher-order cladding mode (7-th), is larger more than an order of magnitude. Therefore, the paradigm that the lower the grating period is, the greater the RI sensitivity is, which is valid for a bulk measurement as already demonstrated [15], is also valid for a surface RI measurement, as occurs in the field of biochemical sensing [3].

A more exact comparison between LPG A and LPG B should have been carried out with gratings having the same thickness of the biolayer, the measurement of which is not simple. On the other hand, results achieved with different LPGs of type A and of type B, not shown, provide values of dynamic signal range comparable with those shown in Table 3 (within 10%). Therefore, although the identity of the thickness of the sensing layers deposited on the two different types of LPG was not measured, the standardization of the protocol in the Eudragit deposition, subsequent surface functionalization and antibody covalent immobilization, as described in Section 2.3, assures that their thicknesses are in the worst case comparable. On this bases, the fact that DSR increases from 28 pm with LPG A to 322 pm with LPG B, with a change of an order of magnitude (exactly of a factor of 11.5) is undoubtedly a sign of a noticeable improvement in the sensitivity of the LPG-based sensor.

It is interesting to observe the effect of the long-term drift on the sensor that translates into reagent concentration measurement error. Clearly, this value

will change with the concentration value, since it depends on the slope of the calibration curve. In fact, the lower the sensitivity is, the lower the slope of the calibration is and, consequently, the greater the reagent concentration measurement error is. Therefore, the errors in correspondence of the minimum (lower bound of the working range = 1.7 mg L^{-1}) and maximum (x_0 = 51 mg L^{-1}) sensitivity of working range were evaluated for LPG B. Considering a drift of 1.5 pm h^{-1}, the related drift-induced errors are 0.15 mg L^{-1} (8.8%) and 1.5 mg L^{-1} (2.9%).

Moreover, it is also worth analysing the kinetics of the interaction between the immobilized mouse IgG antibody and the goat anti-mouse IgG antigen at different concentrations. Figure 13 accounts for the shift of the λ_{res} for the bioassay performed with LPG B as a function of the time at the different concentrations of goat anti-mouse IgG. As in Figure 9, for an easy comparison, the initial value of the λ_{res} is shifted to zero, with the first three experimental data excluded in order to discard the contribution coming from the volume RI change.

All the curves show a typical exponential behaviour with a steady state achieved after 6–8 minutes, proving that the equilibrium in the antibody/antigen interaction is reached. It is important to recall that the measurement was carried out by subsequent addition of goat anti-mouse IgG antigen at increasing concentration. This explains why the shift of the λ_{res} in the presence of the addition of the antigen concentration of 500 mg L^{-1} is lower than the antigen concentration of 100 mg L^{-1}, since at this point the saturation of the antibody/antigen interaction is approaching (as also shown in the calibration curve of Figure 12).

Finally, the specificity of the proposed biosensor was tested for the bioassay performed with LPG B by means of the anti-PSA antibody at a concentration of 10 mg L^{-1}, following the protocol described in Section 2.3. The measured shift of the LPG λ_{res} after the interaction with the anti-PSA antibody with respect to the λ_{res} value recorded in PBS was equal to −0.008 nm. Looking at the calibration curve in Figure 12, this shift is equivalent to the shift caused by the specific antigen at a concentration of 0.2 mg L^{-1}, a concentration 50-fold lower, proving the good specificity of the assay.

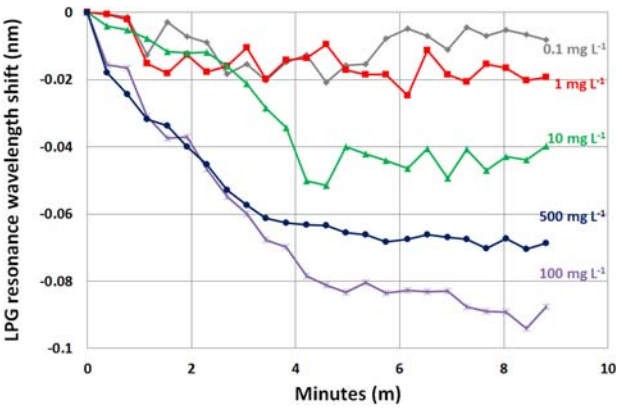

Figure 13 Detail of the goat anti-mouse IgG (antigen) kinetics extrapolated from Figure 8 (LPG B). Comparison between the different antigen concentrations: 0.1 mg L^{-1} (grey rhombuses), 1 mg L^{-1} (red squares), 10 mg L^{-1} (green triangles), 100 mg L^{-1} (violet stars) and 500 mg L^{-1} (blue circles).

4. Conclusion

A complete characterisation of a label-free biosensor based on a long period grating was presented. To the best of our knowledge, this is the first time that the complete calibration curve of a LPG-based biosensor was carried out, thanks to the use of a platform perfectly stabilised and/or automatically compensated in terms of small changes of temperature and strain. The feasibility study of the entire structure was extensively discussed. This study encompassed the experimental evaluation of a novel fibre functionalization chemistry using Eudragit L100 instead of the commonly used silanization procedure, the analysis of the antibody immobilization, the antigen kinetics at different antigen concentrations and the calibration curve of the biosensor in order to extrapolate the metrological parameters.

Experimental results demonstrated an enhancement of the biosensor performance when the fundamental core mode of the single-mode fibre couples with a higher-order cladding mode. Therefore, we experimentally proved that, even if a bare optical fibre is used, the lower the grating period is, the greater the RI sensitivity is, not only for a bulk measurement as already demonstrated [15], but also for a surface measurement as occurs in the field of biochemical sensing [3]. Considering an LPG manufactured on a bare optical fibre, in which the coupling occurs with the 7-th cladding mode, a dynamic signal range of 322 pm, a working range of 1.7–1450 mg L^{-1} and a LOD of 500 µg L^{-1} were achieved. These results are comparable with the results achieved with other LPG-based biosensors (see Table 1 in [3]), although the absence of any temperature and/or strain control in almost all the LPG-based biosensors described in literature makes the achieved results questionable.

It is worth highlighting that there are some of potential further improvements, which could be made in order to enhance the performance of an LPG-based biosensor and to make it comparable with respect to the other label-free optical approaches concerning the biochemical sensing. The most promising methodology is undoubtedly the one that makes use

of LPGs coated with an overlayer RI higher than that of the fibre cladding and working in modal transition. In fact, this approach allows to tune the maximum RI sensitivity near the RI of water and thus near the RI of most biochemical solutions (i.e. SRI = 1.333–1.4 RIU), and hence to reach tremendous values of volume RI sensitivity and resolution in water environment, such as 9000 nm RIU^{-1} and 10^{-6} RIU respectively [27]. Considering that our LPG B is characterised by a volume RI sensitivity of 15 nm RIU^{-1}, the use of LPGs coated with high refractive index layer in our thermo-stabilised flow cell and the adoption of our established bioassay protocol would imply a noticeable improvement in the biosensor performance and an improvement of about two order of magnitude in the value of the limit of detection could be reasonably expected.

Author biographies Please see Supporting Information online.

References

[1] J. Homola, Chem. Rev. **108**, 462–493 (2008).
[2] X. Fan, I. M. White, S. I. Shopova, H. Zhu, J. D. Suter, and Y. Sun, Anal. Chim. Acta **620**, 8–26 (2008).
[3] F. Baldini, M. Brenci, F. Chiavaioli, A. Giannetti, and C. Trono, Anal. Bioanal. Chem. **402**, 109–116 (2012).
[4] M. P. DeLisa, Z. Zhang, M. Shiloach, S. Pilevar, C. C. Davis, J. S. Sirkis, and W. E. Bentley, Anal. Chem. **72**, 2895–2900 (2000).
[5] P. Pilla, P. F. Manzillo, V. Malachovska, A. Buosciolo, S. Campopiano, A. Cutolo, L. Ambrosio, M. Giordano, and A. Cusano, Opt. Express **17**, 20039–20050 (2009).
[6] A. V. Hine, X. Chen, M. D. Hughes, K. Zhou, E. Davies, K. Sugden, I. Bennion, and L. Zhang, Biochem. Soc. Trans. **37**, 445–449 (2009).
[7] V. Mishra, N. Singh, U. Tiwari, and P. Kapur, Sens. Actuators A **167**, 279–290 (2011).
[8] P. Pilla, A. Sandomenico, V. Malachovská, A. Borriello, M. Giordano, A. Cutolo, M. Ruvo, and A. Cusano, Biosens. Bioelectron. **31**, 486–491 (2012).
[9] Z. Wang, J. R. Heflin, K. Van Cott, R. H. Stolen, S. Ramachandran, and S. Ghalmi, Sens. Actuators B **139**, 618–623 (2009).
[10] M. Smietana, W. J. Bock, P. Mikulic, A. Ng, R. Chinnappan, and M. Zourub, Opt. Express **19**, 7971–7978 (2011).
[11] A. M. Vengsarkar, P. J. Lemaire, J. B. Judkins, V. Bhatia, T. Erdogan, and J. E. Sipe, J. Lightwave Technol. **14**, 58–65 (1996).
[12] K. O. Hill and G. Meltz, J. Lightwave Technol. **15**, 1263–1276 (1997).
[13] T. Erdogan, J. Opt. Soc. Am. A **14**, 1760–1773 (1997).
[14] A. N. Chryssis, S. S. Saini, S. M. Lee, H. Yi, W. E. Bentley, and M. Dagenais, IEEE J. Sel. Top. Quantum Electron. **11**, 864–872 (2005).
[15] H. J. Patrick, A. D. Kersey, and F. Bucholtz, J. Lightwave Technol. **16**, 1606–1612 (1998).
[16] S. W. James, N. D. Rees, G. J. Ashwell, and R. P. Tatam, Opt. Lett. **27**, 686–688 (2002).
[17] I. Del Villar, I. R. Matias, F. J. Arregui, and P. Lalanne, Opt. Express **15**, 56–69 (2005).
[18] C. Trono, F. Baldini, M. Brenci, F. Chiavaioli, and M. Mugnaini, Meas. Sci. Technol. **22**, 075204 (2011).
[19] T. Eftimov, in: Optical Guided-wave Chemical and Biosensors II, edited by M. Zourob, A. Lakhtakia, and O. S. Wolfbeis, Springer Series on Chemical Sensors and Biosensors, Vol. 8 (Springer Berlin, Heidelberg, 2010), pp. 151–176.
[20] S. Soria, F. Baldini, S. Berneschi, F. Cosi, A. Giannetti, G. Nunzi Conti, S. Pelli, G. C. Righini, and B. Tiribilli, Opt. Express **17**, 14694–14699 (2009).
[21] J. Cordek, X. Wang, and W. Tan, Anal. Chem. **71**, 1529–1533 (1999).
[22] K. O. Hill and G. Meltz, J. Lightwave Technol. **15**, 1263–1276 (1997).
[23] X. Shu, L. Zhang, and I. Bennion, J. Lightwave Technol. **20**, 255–266 (2002).
[24] R. A. Dudley, P. Edwards, R. P. Ekins, D. J. Finney, I. G. McKenzie, G. M. Raab, D. Rodbard, and R. P. Rodgers, Clin. Chem. **31**, 1264–1271 (1985).
[25] C. Albrecht, N. Kaeppel, and G. Gauglitz, Anal. Bioanal. Chem. **391**, 1845–1852 (2008).
[26] J. Inczedy, T. Lengyel, and A. M. Ure, Compendium of analytical nomenclature. The orange book, 3rd edn. (Blackwell, Oxford, 1998).
[27] P. Pilla, C. Trono, F. Baldini, F. Chiavaioli, M. Giordano, and A. Cusano, Opt. Lett. **37**, 4152–4154 (2012).

